C. R. Physique 3 (2002) 1361–1374

Physique appliquée/*Applied physics*

DOSSIER

MÉCANISMES PHYSIQUES DU NUAGE D'ORAGE ET DE L'ÉCLAIR
THE PHYSICS OF THUNDERCLOUD AND LIGHTNING DISCHARGE

The control of lightning using lasers: properties of streamers and leaders in the presence of laser-produced ionization

François Vidal [a], Daniel Comtois [a], Henri Pépin [a], Tudor Johnston [a], Ching-Yuan Chien [a], Alain Desparois [a], Jean-Claude Kieffer [a], Bruno La Fontaine [a], François Martin [a], Farouk A.M. Rizk [b], Hubert P. Mercure [b], Carl Potvin [b]

[a] **INRS-Énergie, matériaux et télécommunications, 1650 boulevard Lionel-Boulet, Varennes, Québec J3X 1S2, Canada**

[b] **IREQ, Hydro-Québec, 1800 boulevard Lionel-Boulet, Varennes, Québec J3X 1S1, Canada**

Note presented by Guy Laval.

Abstract This paper summarizes the research this team has performed over the past few years investigating laboratory electrical breakdown discharges in the presence of a plasma cylinder created by a single ultrashort laser pulse. This work is part of a feasibility study about the control of lightning using laser systems. Our experimental investigations have included discharges (i) in modest (30 cm) air gaps mediated by streamers, and (ii) in large (several meters) ambient air gaps for which the discharge took place through the formation of a leader, the mechanism relevant to large scale natural discharges such as lightning. In order to understand the observations, various physical models have been used, the main results of which are discussed in this paper. ***To cite this article: F. Vidal et al., C. R. Physique 3 (2002) 1361–1374.***

electrical discharges / leaders / streamers / laser-induced ionization

Le contrôle de la foudre au moyen de lasers : propriétés des streamers et des leaders en présence d'ionisation induite par laser

Résumé Cet article résume les recherches que cette équipe a effectuées au cours des quelques dernières années concernant les décharges électriques en présence d'un cylindre de plasma, créé par une impulsion laser ultra-courte. Ce travail fait partie d'une étude de faisabilité sur le contrôle de la foudre au moyen de systèmes laser. Nos études expérimentales ont porté sur les décharges (i) dans de petits intervalles d'air (30 cm) où le claquage s'effectue par l'intermédiaire de streamers seulement et (ii) dans de grands intervalles d'air (plusieurs mètres) dans lesquels les décharges développent une phase leader similaire à celle observée dans le cas de l'éclair. Dans le but d'interpréter nos observations, plusieurs modèles physiques ont été élaborés, dont les résultats sont discutés dans cet article. ***Pour citer cet article : F. Vidal et al., C. R. Physique 3 (2002) 1361–1374.***

E-mail address: vidal@inrs-ener.uquebec.ca (F. Vidal).

S1631-0705(02)01411-1/REV

décharges électriques / leaders / streamers / ionisation induite par laser

1. Introduction

The use of lasers to investigate electrical discharges dates back to the mid-1960s [1–5] almost at the same time as the laser technology has become widely available, producing pulses of nanoseconds or longer. By ionizing the medium in which they propagate, laser pulses can trigger the discharge at a lower voltage than in the unperturbed medium and guide it along the path of the laser pulse. It was then appreciated that laser pulses, by allowing a control of the physical properties of the medium in which the discharge takes place, constitute a unique tool to enrich our knowledge and improve our understanding of electrical breakdown phenomena.

Soon, the idea has emerged that lasers could be used to guide and to trigger natural lightning [6,7]. This potential application has motivated most research in the field of laser-triggered discharges in the past few years due to the high interest of the electricity utility companies in lightning protection.

Much effort has been devoted to this end in Japan beginning from the early 1990s using relatively long laser pulses (i.e., several nanosecond duration) in the infrared or in the ultraviolet spectrum [8–12]. A research team in Osaka has even reported a successful attempt to trigger natural lightning in real conditions using 2-kilojoule infrared laser pulses [10].

The main drawback of long laser pulses (especially in the infrared spectrum) is that local electron avalanches have time to take place, producing considerable ionization, to the point that the laser pulse is refracted outward, reducing its intensity and bringing the process to a close. With enough energy, the laser-ionized channel appears as a succession of beads in each of which intense ionization takes place. The use of such laser systems to create long ionized channels is thus rather costly from an energetic point of view and requires heavy equipment and high voltage devices.

In 1995, investigations on the propagation of ultrashort laser pulses in ambient air (i.e., $\sim$1 picosecond duration or smaller) showed that, in contrast to nanosecond pulses, long continuous ionized channels could be produced using little laser energy (less than 1 J) and compact laser systems [13]. For such short laser pulses, electron avalanches do not have time to form. However, at such short pulse duration the intensities for the same pulse energy become very high and ionization can take place directly from the laser field. The pulses are seen to propagate for remarkable distances (far greater than the typical Rayleigh length for linear focusing), as a consequence of a balance between the plasma defocusing effect and confinement due to the intensity-dependent part of the index of refraction of air molecules. Our own experiments have shown that short laser pulses could propagate in air for distances of at least 300 m [14]. Due to these particular features, ultrashort laser pulses have been rapidly perceived as a promising alternative way to guide electrical discharges over long distances without the drawbacks of the large laser systems [15].

Starting with this concept, we have undertaken original investigations on the ability of ultrashort laser pulses to trigger and guide electrical discharges in gaps ranging from 30 cm (parallel plane electrodes) to 7 m (from the tip of a 3.7 m rod electrode to the ground plane). As is well known, discharges in air gaps smaller than $\sim$1 m at atmospheric pressure take place through the streamer mechanism. In larger gaps and in non-uniform fields either the streamer mechanism or the leader mechanism can take place [16,17]. In close relation with the experimental program, we have undertaken numerical modeling of several aspects of the phenomena involved, in order to improve our understanding of the observed phenomena. This paper discusses the main results of our investigations for both discharge mechanisms.

The paper is organized as follows. The next section deals with streamer discharges produced in the uniform electric field of a 30 cm air gap at reduced pressures in a conventional laboratory at INRS, using a local short-pulse laser system. Section 3 describes the results obtained with leader discharges obtained in air gaps of several meters in rod-plane geometry in the High Voltage Test Laboratory of Hydro-Québec at

Varennes, with a shielded laser specially installed outside the high-voltage test area. Section 4 deals with the modeling of the leader transition region. The paper ends at Section 5 with a general discussion and summary.

2. Streamer discharges

Although our interests were primarily in leader discharges several meters in length, because of potential applications to the control of natural lightning, in order to establish workable procedures we started our investigations on a simpler, smaller and more accessible system at INRS. We used laser-triggered discharges with 30 cm gaps in a nearly uniform electric field between two parallel electrodes at reduced pressures and with modest voltages which were readily available. With these choices, the discharges obtained were naturally streamers of modest scale rather than the large-scale leaders which were our ultimate interest. Apart from testing the developments for the large-scale system, the results are important for their own worth and even more so because the triggering of streamers is an unavoidable step in the formation of a leader stem.

In this section, we will emphasize two discharge topics. The first is the formation of positive streamers from the laser-created plasma. We shall see that the streamers are generated through the mechanism of local field enhancement due to the charged particle separation at the plasma edges. The second topic is the influence of the laser pulse energy E_L on the threshold electric field necessary to trigger the breakdown. We shall see that the laser pulse energy influences the triggering of streamers through two key parameters: (i) the plasma electron density per unit length N_e, and (ii) the effective electric field $E/(n_h/n_0)$, where E is the electric field and n_h/n_0 is the ratio of the air density to the usual atmospheric values.

The experimental setup used for these experiments is shown in Fig. 1 [18,19]. Two 50 cm diameter plane circular electrodes separated by 30 cm were placed in a chamber in which the gas pressure could be adjusted. A laser pulse of 0.5 ps duration and a wavelength of 0.526 μm and energy up to 120 mJ incident through a 2 cm diameter central hole in the ground electrode was focused on the system midway between the two electrodes. The diameter of the laser pulse at the focus lens was ∼3 mm and the focal length was 50 cm. A double exponential positive voltage pulse was applied to the high voltage electrode with a rise time of ∼0.6 μs and a time to half-value of ∼50 μs. The experiments have been performed in dry air at 350 Torr. Because of the short duration of the laser pulse and its high intensity, the laser pulse focused between the electrodes produces a high-density plasma in the vicinity of the focal point mainly through the mechanism

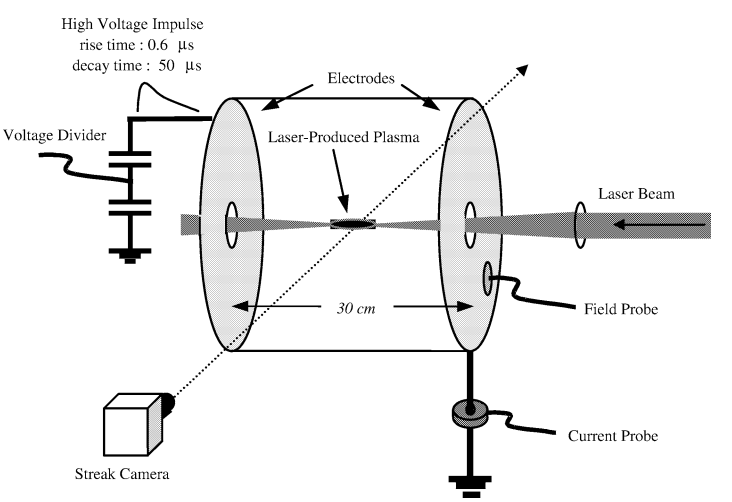

Figure 1. Schematic of the experimental setup. The high-voltage circuit comprises two capacitors that are charged in parallel up to 140 kV and then discharged in series to provide pulses of up to 280 kV, with a rise time of 0.6 μs and a fall time of 50 μs. The high-voltage discharge cell is composed of two parallel electrodes separated by 30 cm. The laser beam is focused between these plates, through small holes, by using a lens with a focal distance of 50 cm. A streak camera records the image of the electrical discharge.

of laser-induced photo-ionization of the ambient gas [20]. The plasma itself is heated mainly through the mechanism of dissociative electron-ion recombination in which a significant part of the laser energy initially spent in ionization is converted into kinetic energy of the fragments of the dissociated molecules. This energy will lead to significant expansion of the plasma typically ∼1 ns after the laser pulse has passed.

An example of streak picture of a discharge performed in dry air at 350 Torr using a laser pulse of 120 mJ is shown in Fig. 2(a). The shape of the voltage pulse is also shown in Fig. 2(b). In the present case, the laser pulse was launched 10 µs before the start of the applied voltage pulse. The maximum of the applied electric field is ∼4.7 kV·cm^{-1}, which is about 40% of the value of the natural breakdown threshold in dry air (∼26 kV·cm^{-1}·atm^{-1}). The white traces on streak image show the light emitted from places where the electric field is high enough to excite the gas significantly. The laser-produced plasma, located near the horizontal center of the streak image (the focal point) is invisible in the picture because the electric field is small in this conductive medium. One observes that ∼0.25 µs after the start of the voltage pulse, sharp luminous traces reach the cathode, starting with a velocity of ∼10^5 m·s^{-1} and accelerating to ∼10^6 m·s^{-1}, reach the cathode. These traces are due to the intense electric field at the head of positive streamers (i.e., those which travel in the direction that would be taken by positively charged particles). At almost the same time as the connection of the first positive streamers to the cathode, one observes a slower luminous trace starting from the opposite edge of the laser-ionized region (the length of which is ∼5–10 cm) and moving toward the anode, which can be identified as a negative streamer. As the negative streamer propagates, new positive streamers are regularly launched on the other side of the plasma channel. The breakdown of the gap generally occurred shortly after the negative side of the plasma had reached the anode [19]. We have observed that the production of the first positive streamers is a necessary and (nearly always) sufficient condition for breakdown.

We believe that, after the connection of the first positive streamers to the cathode, a significant field enhancement then occurs at the anode end of the laser-created plasma (due to their connection via the continuous conductive channel formed by the positive streamers and laser-induced plasma) which

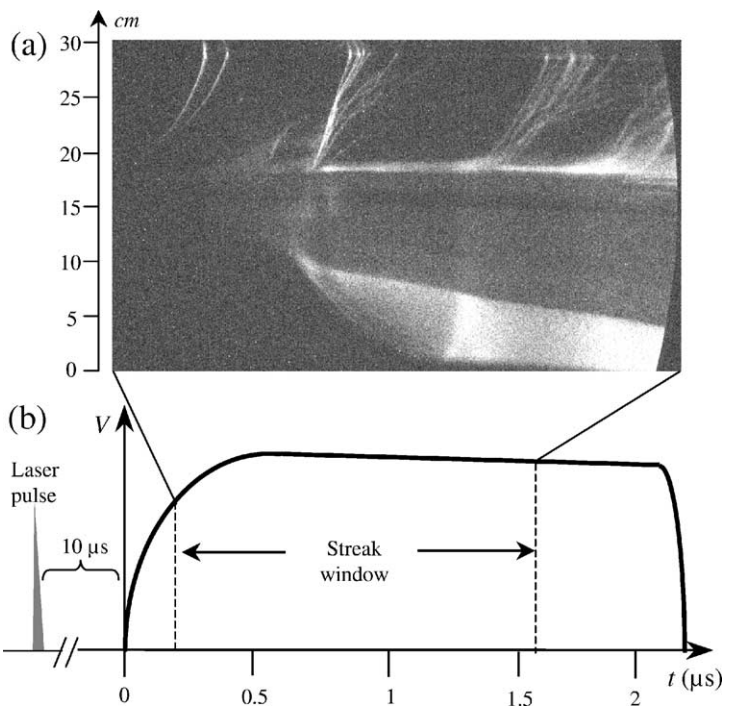

Figure 2. Streak image of the laser-initiated discharge in air, at a pressure of 350 Torr, with a laser pulse energy of 120 mJ. (a) Image of the streamers taken in streak mode. The laser pulse has been launched 10 µs before the start of the voltage pulse. The cathode and the anode are located at the top and at the bottom of the picture respectively. (b) External electric field applied to the gap. The maximum voltage is 140 kV.

causes the triggering of the negative streamers. The fact that this field enhancement mechanism was necessary to launch the negative streamers is due partly to the higher threshold required by negative streamers [16] and, as discussed below, partly to the smaller electron density gradient on the anode side.

In order to understand how the streamers are generated from the laser-created plasma, we have developed a numerical model describing the evolution of the plasma subjected to a time-dependent external electric field [18]. The equation of continuity for the electrons, positive ions and negative ions have been solved along the axis of the plane electrodes for a given plasma width by taking into account electric field ionization, electron–ion recombination, electron attachment with oxygen, and ion–ion recombination. The initial plasma conditions have been obtained using a simple geometrical propagation model for the laser pulse and by using the theoretical rate of photo-ionization [20].

The mechanism of streamer formation resulting from the model is as follows. Due to the fast electron–ion recombination, the initial plasma electron density can be represented roughly as a trapezium with a flat central part and two different inclined edges. On the influence of the external electric field, the plasma particles with opposite charges move in opposite directions, leaving a local net charge, which creates a local electric field. Since no net charge is left in the flat part of the plasma profile, the local field essentially lies at the plasma edges and is even more significant when the electron density gradients at the edges are higher. When the appropriate conditions are met (amplitude of the external electric field, electron density, density gradient, width of the edges, etc.), electron avalanches take place at the plasma edges, leading to the onset of a streamer propagating along the axis toward the nearest electrode. It must be emphasized that the plasma case is nothing like that of a floating metallic electrode where, because of its high conductivity, the skin depth is small compared with the width, and thus the external electric field is excluded. Because the metal conductivity is so high its value becomes irrelevant and we are left with a geometric field concentration effect due to the shape and placement of the conductor. In the laser-induced plasma case, the electron density is sufficiently low that the skin depth is large and the external electric field penetrates easily. Thus significant modification of the externally imposed electric field here only occurs at the ends of the plasma, where there are high local electric fields due to charge separation. Unlike the conductor case, the effect is directly proportional to the electron density per unit length.

The experiments have shown that the minimum electric field required to trigger the breakdown can be significantly reduced by increasing the laser pulse energy [19]. For example, in the experiments performed in air at 350 Torr, when the laser pulse is launched nearly in coincidence with the maximum voltage, threshold electric fields of $\sim$5.6 kV·cm^{-1}, $\sim$4.6 kV·cm^{-1} and $\sim$3.2 kV·cm^{-1} (the natural breakdown value being $\sim$12 kV·cm^{-1}) have been obtained for laser pulse energies of 15 mJ, 35 mJ and 120 mJ respectively.

From the theoretical investigations it has been concluded that the influence of the laser energy on the triggering of streamers can be usefully described by means of two main parameters [21]:

(i) The first parameter is the electron density per unit length $N_e = n_e \pi R_p^2$ (where n_e is the average electron density per unit volume and R_p is the plasma radius) of the plasma near the focal point. In [21] it has been shown that N_e increases with the laser pulse energy. Besides, using the above mentioned numerical model for the onset of streamers [18], we have shown that the local electric fields induced by charge separation at the plasma edges increase significantly with both R_p and n_e, [19] and thus with the laser pulse energy. As discussed above, high local electric fields at the plasma edges can induce streamers, which is a necessary condition for breakdown.

(ii) The second parameter is the effective electric field $E_{\text{eff}} = E/n_h$ (n_h being the air density). As the laser pulse energy increases, more energy per unit volume is deposited in the plasma, causing its thermal expansion and thus the increase of the effective electric field E_{eff}. As is well-known, most electric field-dependent reactions in the plasma depend on E_{eff} instead of E alone [16]. Therefore, the decrease of the air density n_h due to thermal expansion (from conversion of ionization energy to plasma thermal energy and thus pressure) can enhance sufficiently the effect of the applied electric field to actually ionize the

plasma and thus to increase the electron density per unit length N_e. (The induced expansion also probably enhances the effect of the local electric field at the plasma edges.) There is, however, a characteristic cooling time τ_{th} of the plasma-heated and expanded region, given by $\tau_{th} \sim R_p^2/4\kappa_h$, where κ_h is the air thermal conductance. After this time the plasma contracts back to its initial volume as its temperature drops by thermal conduction towards the temperature of the ambient medium. As shown in [21], this time scale characterizes the maximum delay between the laser pulse and the voltage pulse for which streamers can be triggered below the natural breakdown threshold.

3. Leader discharges

Since our main interest is the control of natural lightning by lasers, we have devoted the greater part of our efforts to understand the leader triggering and guiding properties of long laser plasma channels in long air gaps (3–7 m) where stable and free propagation of leaders can take place. Our approach was to characterize experimentally the evolution of discharges, with and without a laser plasma, and to apply to these the model of the positive discharge in long air gaps as elaborated by Bondiou and Gallimberti [22]. We have studied two rod-plane configurations. In one (classical), a positive high voltage pulse is applied to the rod electrode placed above the ground plane [23,24]. In the other (non-classical) configuration, the rod is placed on the ground plane and a negative high voltage pulse is applied to a large plane above [25].

In this section we will present results of the 7 m gap in the classical rod-plane configuration and show that we can describe adequately the leader discharge in presence of a laser plasma channel by using the Bondiou–Gallimberti model. We have observed experimentally that the linear charge q_L of a positive leader is significantly smaller, compared to its ordinary value, when it develops along a laser-created plasma channel. In the model, q_L is a parameter which determines the rate of leader growth, linking its velocity v_L with the current input I_L produced by the progression of the corona front through the relation $v_L = I_L/q_L$. We have observed that the effect of a laser-produced plasma on the discharge can be accounted for in the Bondiou–Gallimberti model by simply reducing the value of q_L over the laser plasma channel length.

The experiments have been performed at the Hydro-Québec High-Voltage Laboratory. In our experimental classical setup, shown in Fig. 3, a circular 15-meter diameter ground plane electrode, with a central hole for laser beam propagation, is located 3 m above the floor. The top electrode is a 3.7 m rod (diameter 6 cm) with a 12 cm diameter sphere at its tip, attached at the center of a 5 m diameter electrode. (This top electrode is far enough from the gap to have a negligible influence on the electric field distribution.) A high voltage (HV) generator was used to apply a positive voltage pulse to the rod electrode, with a critical rise time of 270 μs matched to the gap length. The time to half-value of the applied voltage pulse was 2.5 ms. Because of the necessity of leaving the high-field region completely clear and to avoid the interference to the laser system from the high-voltage power system operation, the laser system was placed in a shielded room outside the high voltage test, some 30 meters distant. We used a BMI-Thomson Ti: sapphire laser system ($\lambda = 800$ nm, minimum pulse duration $= 60$ fs, maximum energy in the laser pulse after compression $= 500$ mJ). An image-relay system enclosed in near-vacuum (10^{-5} Torr) transferred the beam from the laser room to the test site (below the ground electrode). The beam had an elliptical shape with principal axes of 4.5 cm and 3.2 cm. We used lenses of various focal lengths (4.7 m to 8.8 m) to focus the laser beam approximately 30–40 cm below the sphere at the tip of the top electrode. The minimum pulse duration (measured by second order autocorrelation) that was used in these experiments was around 0.6–1 ps corresponding, with our optical arrangement, to the appearance of white light on the surface of the focussing lens (threshold of damage on this lens).

An example illustrating the dynamics of a laser-induced discharge appears in Fig. 4. We present a streak record, the leader current and the corresponding HV pulse. For this event, the plasma was produced with a 200-mJ laser pulse and the plasma channel length was ∼3.5 m. The laser beam was launched about 30 μs after the start of the voltage pulse, which had a peak amplitude of 1600 kV. With the laser-produced

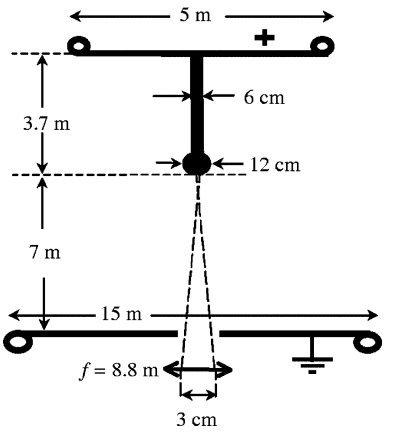

Figure 3. Experimental setup for leader discharges.

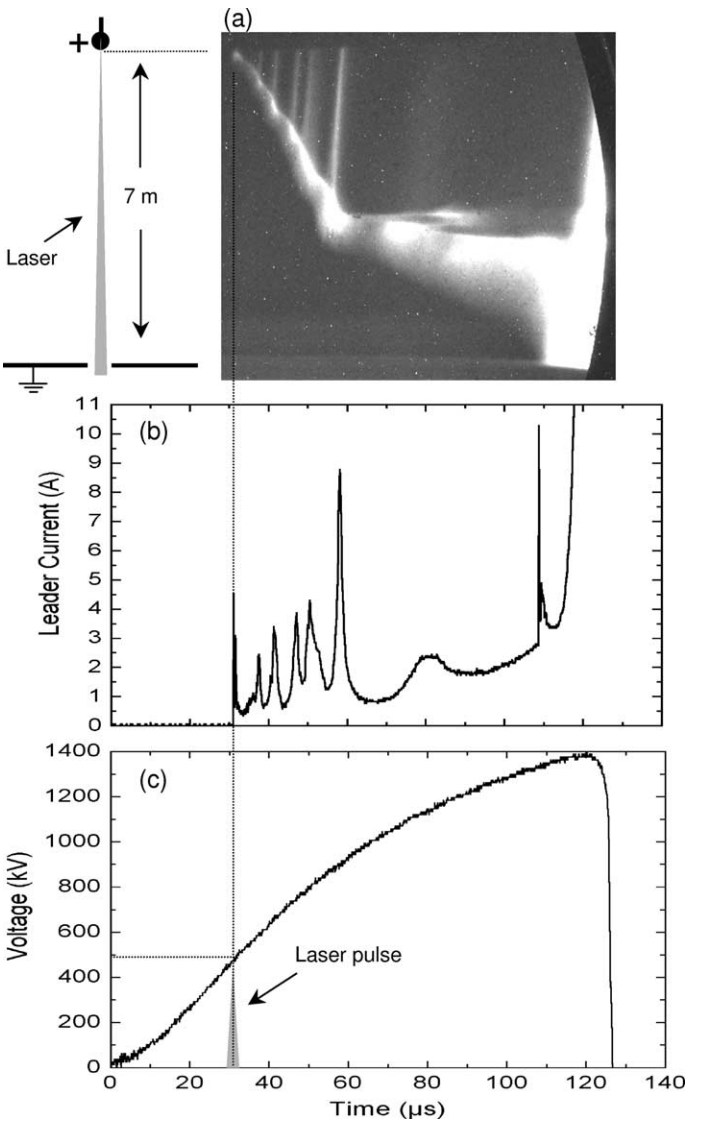

Figure 4. Example of results of a laser-guided discharge: (a) streak picture of the development of the leader; (b) current record; (c) voltage pulse applied to the cathode.

plasma we inferred from the streak images a very large effective leader velocity of about 10^5 m·s^{-1}, a value which is ten times that of a natural leader. In the case shown the leader traveled in the gap at the increased velocity up to the point where it left the laser-produced plasma, continuing its propagation at the usual 'natural' velocity of about 10^4 m·s^{-1} up to the final jump. In contrast to the rather erratic motion of leaders in normal conditions, the leader was guided by the laser-created plasma and followed a perfect rectilinear trajectory. As the leader propagated in the plasma created by the laser, the current measured at the HV rod electrode showed strong fluctuations correlated with the vertical spikes in the streaked images. We believe that these strong and irregularly-occurring current pulses observed during guided leader propagation can be interpreted as *restrikes*, since the leader grows too fast compared to the rate at which the applied voltage increases. The average current of the laser-guided leader (1.4–1.8 A) was higher than that measured in the case of the natural discharge without laser channel (0.6–0.8 A). By integrating the current waveform, we could measure the leader charge as a function of its length. We inferred in this case a linear charge density of approximately 15 μC·m^{-1} (lower than the 40 μC·m^{-1} for a natural leader development [26]) to sustain the guided propagation of the leader in the plasma channel. The lower amount of charge per unit length and the higher average current leads naturally to a leader velocity of $(v_L = I_L/q_L) \sim 10^5$ m·s^{-1}. The amount of leader current charge required to generate a unit leader length (q_L) in presence of a laser channel indicates that this channel improved the efficiency of the corona-leader transition.

Let us point out that there are other striking differences between the guided and the natural discharges. In the guided discharge, there is no statistical delay for the inception of the first corona, as early free electrons are provided by the laser pulse via photo-ionization. Also, there is no (or at most a very short) dark period, so that the leader inception voltage is much lower. By firing the laser early with respect to the voltage pulse, the leader inception voltage can be as low as 300 kV, which corresponds to a reduction of more than 50% of the average normal leader inception voltage (without the laser) in our experimental conditions. All this consistently indicates that the laser plasma is indeed providing a conduction path that facilitates the initiation of the leader. It is also interesting to note that the breakdown voltage of the gap (U_{50}) is lowered when the leader is laser-guided, depending on the length of the laser plasma channel. In the experimental conditions described, it is seen on Fig. 4 that the breakdown voltage is 1400 kV for a plasma channel length of 3.5 m, whereas the natural breakdown voltage is 1600 kV.

We have used the Bondiou–Gallimberti model [22] to compute the development of the discharge in presence of the laser plasma channel. The numerical simulations have been done for a 7 m gap, with the same electrode configuration as in the experiments. The voltage pulse reproduces the one used in the experiments. As remarked above, the effect on the leader of the laser-created plasma can be simply taken into account in the model by changing q_L to the value necessary to give the experimentally measured value for the leader velocity. There seems no need to change anything else in the model to reproduce the leader propagation. Fig. 5 presents a simulation with a laser plasma channel of 3.5 m. In order to reproduce the starting conditions in presence of the laser, we impose in the simulation the inception of the corona-leader mechanism at a given time corresponding to the firing of the laser. As remarked above, the laser-created plasma is taken into account in the simulation by simply lowering q_L (compared to the natural case) over a distance of 3.5 m. The value of q_L associated with the presence of the laser-produced plasma is $\sim$10 μC·m^{-1}. Fig. 5 shows the same features as Fig. 4: the leader velocity in the channel is $\sim 10^5$ m·s^{-1} and $\sim 10^4$ m·s^{-1} outside the channel; the leader corona extension (between the leader tip and the corona head) associated with the propagation in the plasma channel is narrower than for the natural propagation; the final jump occurs at a time of $\sim$130 μs at a voltage of 1400 kV. The average leader current of 1 A is close to the experimental average value of 1.6 A. However, the steadily-moving leader propagation model of Bondiou and Gallimberti is not able to reproduce the restrikes and the strong fluctuations of current that are seen experimentally (Fig. 4) during the guided leader propagation.

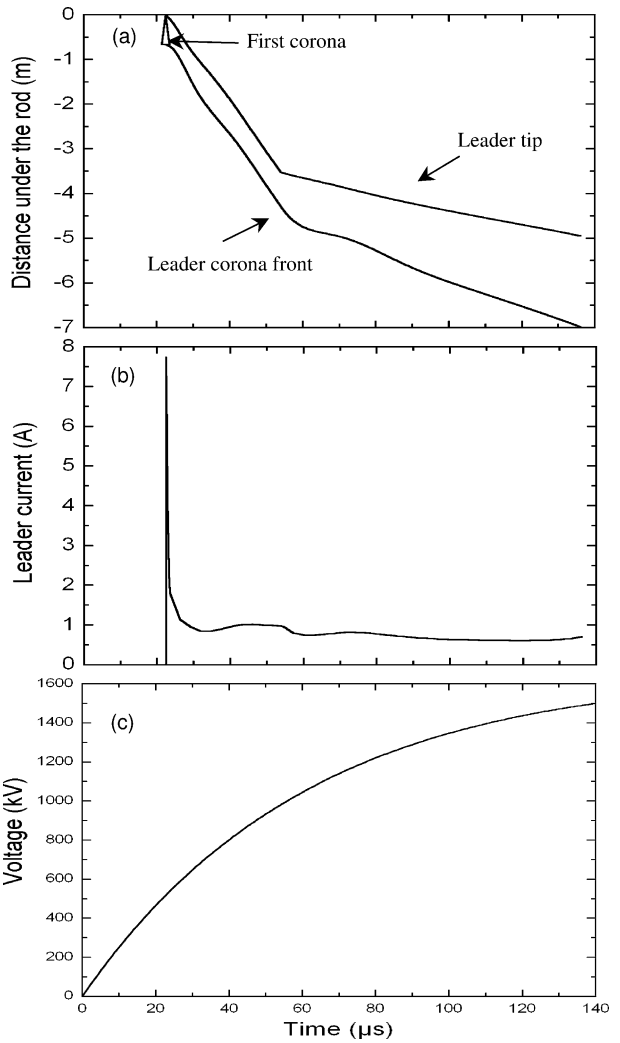

Figure 5. Results of simulations of a laser-guided discharge, computed with a q_L value of 10 μC·m^{-1} on a distance of 2 m above the rod, in order to represent the effect of the laser-created plasma channel. (a) Computed streak picture. (b) Computed current. (c) Voltage pulse applied to the cathode.

4. Modeling the positive leader transition region

In order to understand the effects of the laser-ionized channel in leader discharges, we have undertaken the modeling of the leader transition region, in which new portions of the leader are formed, and which separates the ambient medium from the main body of the leader. Two models are discussed in this section.

The first model discussed is aimed at explaining the reduction of q_L which has been observed in laser-guided leader propagation. The model discussed in Section 4.1 uses the fact that the density of negative ions per unit length N_e is higher in a laser-ionized plasma along the leader's path than in normal conditions. The consequences of the increase of N_e, are that the required temperature in the leader transition region (from which follows a lower value of q_L) is now lower for achievement of the appropriate value for resistance per unit length.

The second model discussed starts from a completely different point of view and has been developed to study the plasma properties within a limited region around the leader tip. In that model, the charged particle densities, the electric field and the air temperature are calculated self-consistently in a two-dimensional geometry with axial symmetry. The model, its main results and its limitations are discussed in Section 4.2.

4.1. Explaining the lowering of q_L

The mechanism described here to explain the lowering of q_L follows the guideline of the model proposed by Gallimberti [26] (a component of the Bondiou–Gallimberti model [22]) for leaders propagating in normal conditions (without laser-ionized channel). According to that model, the appropriate conductivity in the transition region is achieved by detaching the electrons from the negative ions of the leader's path. (Due to the high electron mobility, the detached electrons increase considerably the conductivity.) The negative ions in the streamer filaments (the part in contact with the leader region) result from the rapid attachment (in only $\sim 10^{-8}$ s) of the electrons initially generated in the streamer heads. The same applies to the plasma generated some time earlier by the short-pulse laser. In the leader transition region, the electron detachment necessary to advance the leader is presumed to be achieved by heating the air to a temperature of $\sim$1500 K through collisions of the neutral air particles with the charged particles accelerated by the electric field at the leader tip.

The starting point of the model presented here is that the density of negative ions per unit length along the leader's path is higher for a laser-ionized channel than for an ensemble of streamer filaments. This assertion is justified as follows. The laser ionized channel is characterized, in our experimental conditions, by an average diameter of $\sim$1 mm and a negative ion density of 10^{12}–10^{13} cm^{-3} [25]. In virgin air a new portion of the leader grows in an ionized channel made of a few streamer filaments. These filaments are characterized by a diameter of 50–100 μm and a negative ion density of 10^{12}–10^{13} cm^{-3} [16]. One concludes that the ratio

$$f = (N_-)_{\text{laser channel}}/(N_-)_{\text{streamer channel}}, \tag{1}$$

where $(N_-)_{\text{laser channel}}$ and $(N_-)_{\text{streamer channel}}$ are the density per unit length of negative ions in the laser-ionized channel and in a streamer-ionized channel respectively, is of the order of the ratio between the cross-sectional areas of the laser-ionized plasma and the streamer-ionized region, i.e., of the order of 10–100.

In order to extend Gallimberti's model to the case of a laser-ionized channel, we first assume that the leader geometry itself and the electric field distribution inside the leader are practically unaffected by the laser-ionized channel. Following this assumption, and neglecting the influence of the leader velocity, the charge per unit length reads simply [26,22]

$$q_L \approx 3.5 \times 10^{-8}(T_c - T_0). \tag{2}$$

The mechanism by which q_L is lowered might well be achieved as follows. In a medium in which a higher density of negative ions per unit length is available, such as in a laser-ionized channel, only a smaller temperature T_c in the transition region has to be achieved. This is because the negative ions themselves contribute significantly to the conductivity so that a smaller fraction of the electrons have to be detached to obtain the appropriate low *resistance per unit length* R. The latter is defined as the reciprocal of the laterally integrated conductivity, and is expressed as

$$R^{-1} = e\mu_e N_e + e\mu_i N_- + e\mu_i N_+. \tag{3}$$

Here μ_e and μ_i are the mobility of electrons and ions respectively, and N_e, N_- and N_+ are the densities per unit length of electrons, negative ions and positive ions respectively. Since the temperature T_0 of the air along the path of the leader depends weakly on the presence of a laser-ionized channel [24], the lowering of q_L thus follows directly from the lowering of the temperature T_c in the transition region.

Quantitative results have been obtained as follows. By assuming that: (i) detachment nearly balances attachment in the transition region (as in Gallimberti's model), and (ii) that the plasma is neutral, one can easily express R as a function of N_- along the leader's path. The temperature T_c as a function of f, Eq. (1), can then be obtained from the condition $R(T = 1500\ \text{K}) = R(T_c)$.

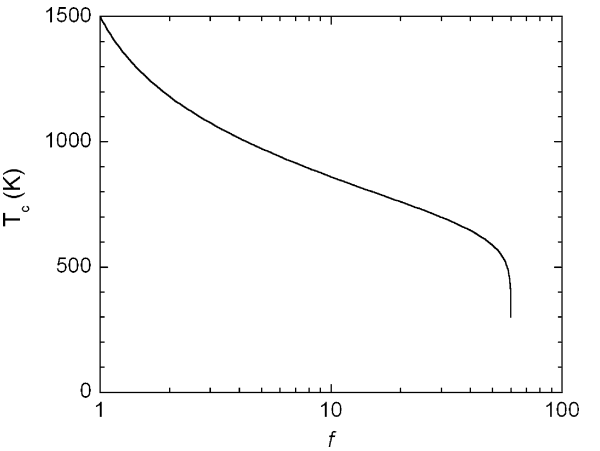

Figure 6. Critical temperature of the transition region (T_c) as a function of the ratio f between the density of negative ions per unit length of the laser-ionized channel and the natural density of negative ions per unit length due to streamers.

The result is illustrated in Fig. 6 where the temperature T_c is plotted as a function of the ratio f. One observes that the temperature of the transition region decreases as f increases. By definition, the value of $f = 1$ corresponds to a temperature of 1500 K. The temperature vanishes as f approaches the value of $\sim$60 since in that case the negative ions alone can provide the required resistance per unit length and no electron detachment is necessary. Using Fig. 6 and Eq. (2), one finds easily that a value of f between 10 and 50 is needed to obtain the values of q_L observed in experiments for laser-guided leaders (i.e., 10–20 μC/m), in agreement with the estimate made above.

4.2. Two-dimensional model of the positive leader tip

The purpose of the model discussed here [27] is to investigate the properties of the air plasma surrounding the tip of the leader. For simplicity we have assumed that the leader, including most of the transition region, is a perfect conductor having a defined parabolic shape with a radius of curvature of 10 μm at the tip. This simplification allowed us to calculate self-consistently the motion of the charged particles (electrons, positive ions, and negative ions), the electric field and the air temperature in a two-dimensional space, assuming axial symmetry.

The model equations include the following: (i) the continuity equations for the charged species by taking into account the rates of ionization, attachment, detachment, electron-ion recombination and ion–ion recombination; (ii) Poisson equation for the electric field; and (iii) the energy equation for the air temperature in which the source term is the power dissipated by the collisions between the air molecules with the charged particles accelerated in the local electric field. The air density has been assumed uniform and the temperatures of the charged species have been described as simple function of the electric field. The equations have been solved in the frame of reference of the leader tip assumed to evolve with the constant velocity $v_L = 10^4$ m·s^{-1}, which is a typical value for normal leaders. The stationary solutions of the equations of the model have been obtained within a parabolic system of coordinates.

Since the equations have to be solved within a limited domain around the leader tip, reasonable boundary conditions have had to be prescribed in order to make the connection between two disparate domains. These two are: (i) the relatively small calculation domain; and (ii) the rest of the system made up of the electrodes, most part of the leader and the streamer corona. Moreover, since the leader is assumed to be a perfect conductor of parabolic shape, appropriate boundary conditions have also been prescribed at its surface.

The main results of the model can be summarized as follows:

(i) Due to the shielding by the plasma surrounding the tip of the leader, the actual electric field is very different from the bare geometrical field obtained using the same boundary conditions. For the chosen radius of curvature of 10 μm at the tip of the leader, the actual electric field at the tip is about 10^3 times

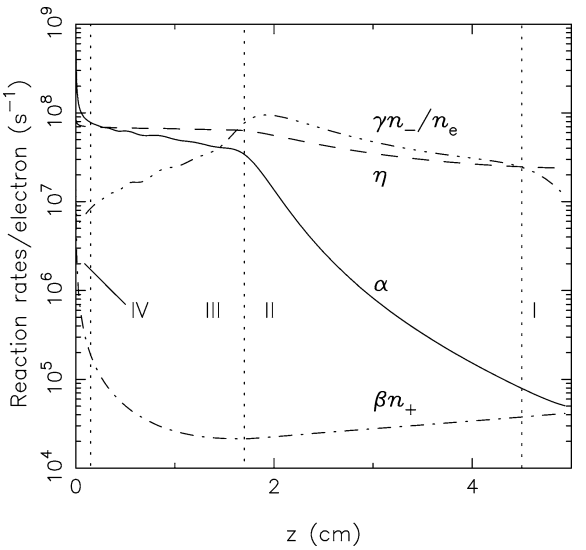

Figure 7. Reaction rates per electron on the axis as a function of the axial position resulting from the two-dimensional model. The tip of the leader is at $z = 0$. (α = ionization, β = ion–electron recombination, γ = electron detachment, η = electron attachment). Vertical dotted lines delimit the four following regions. Region I: non-perturbed ion plasma (outside the leader tip region). Region II: electron multiplication by detachment. Region III: electron-dominated plasma (quasi equilibrium). Region IV: ionization region, transition sheath.

smaller than the bare field, but is relatively enhanced at distances larger than ∼0.15 cm from that point. The electric field, as a function of the axial position, shows four different zones. The field has a maximum of 38 kV·cm^{-1} at the tip and decreases rapidly to ∼20 kV·cm^{-1} within ∼0.15 cm from that point. Over the next ∼1.8 cm, the field remains in the range 18–20 kV·cm^{-1}, which corresponds approximately, in our model, to the field value where ionization and detachment balance attachment and recombination. Beyond ∼1.8 cm, the field decreases to the assigned value of 4–5 kV·cm^{-1}, which corresponds to the field measured in the streamers [28].

(ii) Fig. 7 shows the various reaction rates per electrons as a function of the axial position as obtained from the model. For a distance smaller than ∼0.1 cm from the tip, ionization is the most important process (region I), while farther from that point, where the field is still modest, detachment is more important than ionization and attachment (region III). There is an intermediate region where attachment is the dominant process (region II). Electron–ion recombination is always negligible. Electron detachment from negative ions thus plays an important role in the charged-particle dynamics in front of the leader, as hypothesized in the model discussed in Section 4.1 and in [26]. However, detachment, while important, is not the dominant source of electrons everywhere, since ionization becomes very significant close to the leader tip, where the electric field has the largest amplitude.

(iii) A leader current of 0.21 A has been obtained, which is the correct order of magnitude for leader in normal conditions although it is somewhat smaller than most measurements (∼0.5–1.0 A). (We suspect that the current would be larger if the calculation domain was to include a longer portion of leader, limited here by computer restrictions.)

(iv) Contrary to some expectations, the air heating obtained at the tip is only ∼100 K, which is too small to play any role in the physical processes occurring in the calculation domain.

While the model discussed here provides new insights in the plasma properties near the leader tip, its main shortcoming is that the transition region is treated as a perfect conductor. A more satisfactory modeling of the leader would require taking into account explicitly the gas dynamical processes (i.e., air heating and expansion) taking place in the transition region. Besides, it is not clear whether the space and time average of the streamer field near the tip used in that model would not conceal some important aspect of the leader dynamics. For instance, it is unclear whether there are significant problems which have been simply ignored when one combines ensemble of streamers, each of which is a complicated and very nonlinear plasma object

into an effective mean-plasma model. However, such an improved model would involve difficult conceptual and computational issues that we have chosen to avoid at this stage of our investigations.

A consequence of the 'perfect conductor' assumption made here is likely that the electric field and ionization at the tip are overestimated (despite the observed damping due to space charges) since otherwise the potential would vary more gradually. This lowering of ionization at the tip would be more consistent with the electron detachment models discussed in [26] and in Section 4.1. As a matter of fact, it should be realized that ionization is actually difficult to reconcile with leader transition region models in which detachment plays a central role. This is because ionization alone, if significant enough, could well feed the leader transition region with enough free electrons to achieve the required conductivity. The electron detachment process could then be comparatively negligible.

Finally, let us add that the very low air heating found at the tip in this model probably indicates that the leader heating does not take place suddenly at the tip. The heating is more likely to be distributed more gradually in the transition region (possibly over centimeters), in a way more consistent with the simple model discussed in Section 4.1.

5. Summary and conclusions

This paper has presented experimental and modeling results concerning discharges triggered by focused ultrashort laser pulses. Streamer discharges in 30 cm gaps and leader discharges in gaps up to 7 m have been considered. Our theoretical investigations on the leader transition region have also been discussed in Section 4.

Laser pulses modify the medium in which the discharge takes place through ionization and gas heating. We have observed that in 30 cm plane–plane air gaps at modest pressure (350 Torr) where streamer formation dominates, laser energies of 120 mJ could trigger discharges at only $\sim$25% of the natural breakdown electric field. Streamers are triggered from the edges of the laser-created plasma through the mechanism of local field enhancement due to charge separation. Important plasma parameters are the electron density per unit length N_e and the effective electric field E_{eff}. The typical time by which the heated plasma keeps its ability to trigger streamers below the natural breakdown electric field is given by the thermal conduction characteristic time τ_{th}.

In air gaps of several meters, a single laser pulse has been shown to trigger and guide the leader discharge, and to increase the leader velocity by a factor of ~ 10. Modeling using the Bondiou–Gallimberti model has been shown to provide results in good agreement with the experiments provided the parameter q_L (the charge per unit length) is lowered consistently with the experimental observations. In such large gaps, the heating of the ambient gas by the laser pulse seems to be negligible. The main effect of the laser pulse is likely to increase the density of negative ions per unit length in which the leader propagates. A model of the leader transition region based on this finding and intended to explain the lowering of q_L has been discussed in Section 4.1.

The two-dimensional model of the plasma near the leader tip discussed in Section 4.2 demonstrates that much remains to be learned concerning the mechanisms of propagation of the leader from the point of view of the elementary processes. The assumption made in that model, that most of the transition region is a perfect conductor, because of the high ionization rate obtained at the leader tip, does not seem to be consistent with a simple picture dominated by negative ion density per unit length. It rather seems that an extended transition region in which the conductivity would increase gradually would constitute a more realistic picture of the leader transition region. The self-consistent modeling of the leader transition region still presents major challenges, both conceptual and technical, to the researchers in the field of lightning discharges.

The feasibility study that we have undertaken is encouraging regarding the understanding of the control of lightning by means of lasers. The achievement of this goal could be possible in the near future in view of the rapid development of compact short pulse laser systems.

Acknowledgments. The authors are grateful to Dr. Anne Bondiou-Clergerie and Dr. Philippe Lalande from ONERA, and Dr. Ivo Gallimberti from the University of Padova, for making possible the use of the codes of the Bondiou–Gallimberti model, for helping in the interpretation of the modeling results and for many helpful discussions.

References

[1] W.K. Pendleton, A.H. Guenther, Rev. Sci. Instrum. 36 (1965) 1546.
[2] A.H. Guenther, J.R. Bettis, IEEE J. Quant. Electron. QE-3 (1967) 581.
[3] A.G. Akmanov, L.W. Rivlin, V.S. Shildyaev, JETP Lett. 8 (1968) 258.
[4] R.C. Klewe, M.B.C. Quigley, B.A. Tozer, Appl. Phys. Lett. 15 (1969) 155.
[5] V.I. Vladimirov, G.M. Malyshev, G.T. Razdobarin, V. Semenov, Soviet Phys. Tech. Phys. 14 (1969) 677.
[6] D.W. Koopman, T.D. Wilkerson, J. Appl. Phys. 42 (1971) 1883.
[7] L.M. Ball, Appl. Opt. 13 (1974) 2292.
[8] D. Wang, T. Ushio, Z.I. Kawazaki, K. Matsuura, Y. Shimada, S. Uchida, C. Yamanaka, Y. Izawa, Y. Sonoi, N. Simokura, J. Atmos. Terr. Phys. 57 (1995) 459.
[9] M. Miki, T. Shindo, Y. Aihara, J. Phys. D 29 (1996) 1984.
[10] T. Yamanaka, S. Uchida, Y. Shimada, H. Yasuda, S. Motokoshi, K. Tsubakimoto, Z. Kawasaki, Y. Ishikubo, M. Adachi, C. Yamanaka, Proc. SPIE 3343 (1998) 281.
[11] K. Nakamura, T. Suzuki, C. Yamabe, K. Horii, Elec. Engrg. Japan 114 (1994) 69.
[12] M. Miki, A. Wada, J. Appl. Phys. 80 (1996) 3208.
[13] A. Braun, G. Korn, X. Liu, D. Du, J. Squier, G. Mourou, Opt. Lett. 20 (1995) 73.
[14] B. La Fontaine, F. Vidal, Z. Jiang, C.Y. Chien, D. Comtois, A. Desparois, T.W. Johnston, J.-C. Kieffer, H. Pépin, Phys. Plasmas 6 (1999) 1615.
[15] X.M. Zhao, J.C. Diels, C.Y. Wang, J.M. Elizondo, IEEE J. Quantum Electron. 31 (1995) 599.
[16] Yu.P. Raizer, Gas Discharges, Springer-Verlag, Berlin, 1991.
[17] F.A.M. Rizk, IEEE Power Delivery 4 (1989) 596.
[18] B. La Fontaine, F. Vidal, D. Comtois, C.Y. Chien, A. Desparois, T.W. Johnston, J.C. Kieffer, H.P. Mercure, H. Pépin, F.A.M. Rizk, IEEE Trans. Plasma Sci. 27 (1999) 688.
[19] A. Desparois, B. La Fontaine, A. Bondiou-Clergerie, C.Y. Chien, D. Comtois, T.W. Johnston, J.-C. Kieffer, H.P. Mercure, H. Pépin, F.A.M. Rizk, F. Vidal, IEEE Trans. Plasma. Sci. 28 (2000) 1755.
[20] L.V. Keldysh, J. Exp. Theor. Phys. 47 (1964) 1945.
[21] F. Vidal, D. Comtois, C.Y. Chien, A. Desparois, B. La Fontaine, T.W. Johnston, J.-C. Kieffer, H.P. Mercure, H. Pépin, F.A. Rizk, IEEE Trans. Plasma Sci. 28 (2000) 418.
[22] A. Bondiou, I. Gallimberti, J. Phys. D 27 (1994) 1252.
[23] D. Comtois, C.Y. Chien, A. Desparois, F. Génin, G. Jarry, T.W. Johnston, J.-C. Kieffer, B. La Fontaine, F. Martin, R. Mawassi, H. Pépin, F.A.M. Rizk, F. Vidal, P. Couture, H.P. Mercure, C. Potvin, A. Bondiou-Clergerie, I. Galllimberti, Appl. Phys. Lett. 76 (2000) 819.
[24] H. Pépin, D. Comtois, F. Vidal, C.Y. Chien, A. Desparois, T.W. Johnston, J.C. Kieffer, B. La Fontaine, F. Martin, F.A.M. Rizk, C. Potvin, P. Couture, H.P. Mercure, A. Bondiou-Clergerie, P. Lalande, I. Gallimberti, Phys. Plasmas 8 (2001) 2532.
[25] D. Comtois, H. Pépin, F. Vidal, F.A.M. Rizk, C.Y. Chien, T.W. Johnston, J.C. Kieffer, B. La Fontaine, F. Martin, C. Potvin, P. Couture, H.P. Mercure, A. Bondiou-Clergerie, P. Lalande, I. Gallimberti, Part I (experiments) and Part II (modeling), IEEE Trans. Plasma Sci., submitted.
[26] I. Gallimberti, J. Phys. 40 (1979) 193.
[27] F. Vidal, I. Gallimberti, F.A.M. Rizk, T.W. Johnston, A. Bondiou-Clergerie, D. Comtois, J.C. Kieffer, B. La Fontaine, H.P. Mercure, to be published in IEEE Trans. Plasma Sci., June 2002 issue.
[28] B. Hutzler, D. Hutzler, EDF Bull. Direction Études Rech. Sér. B Réseaux Électriques, Matériels Électriques 4 (1982) 11.